

Journal of
Mechanics of
Materials and Structures

**FRACTURE AND FATIGUE CRACK GROWTH ANALYSIS OF RAIL
STEELS**

Heshmat A. Aglan and Mahmood Fateh

Volume 2, N° 2

February 2007



mathematical sciences publishers

FRACTURE AND FATIGUE CRACK GROWTH ANALYSIS OF RAIL STEELS

HESHMAT A. AGLAN AND MAHMOOD FATEH

Low carbon bainitic steel shows promising potential, especially in critical components such as frogs and switches. Microstructural analysis of J6 bainitic rail steel was performed and compared with the microstructure of premium pearlitic rail steel. The bainitic microstructure revealed a mixture of tempered martensite and ferrite associated with intralath carbides. Typical pearlitic microstructure with a fine lamellar aggregate of very soft and ductile ferrite and very hard carbide cementite was observed. The mechanical properties, plane stress fracture toughness, K_{Ic} , and the fatigue crack growth behavior of the two steels were evaluated. Test specimens were machined from railheads of each material using electrical discharge machining (EDM). Rectangular unnotched and notched specimens were used for the mechanical properties and fatigue evaluation respectively. $1/2T$ compact tension specimens were used for the K_{Ic} evaluation according to ASTM E399. The J6 bainitic steel has ultimate strength, yield strength, and elongation to failure of about 1500 MPa, 1100 MPa, and 13% respectively. These values are higher than those for pearlitic steel. It was found that the average K_{Ic} for the bainitic rail steel is 52 MPa \sqrt{m} , while that of the premium pearlitic steel is 41 MPa \sqrt{m} . Fatigue studies showed that the crack speed for the bainitic steel is lower than that for the pearlitic steel over the entire range of the energy release rate. The bainitic steel exhibits a higher rate of crack deceleration in the second stage, as indicated by the lower slope of the fatigue crack propagation kinetics curve in comparison with the pearlitic steel. This attests to the superior fatigue damage tolerance of the bainitic rail steel and provides evidence to support the superior rolling fatigue damage tolerance of the bainitic rail steel reported in the literature.

1. Introduction

Pearlitic steel accounts for most of the steel tonnage produced today [Smith 2004, 427–522]. Bainitic steel can offer some advantages compared to standard pearlitic steel in special track applications, for example, high angle crossing diamonds [Davis et al. 2002]. Recent studies reported in [Kristan 2005] have shown that J6 bainitic rail steel in a revenue service trial has shown performance superior to standard head-hardened pearlitic steel. A 50% reduction in rolling contact fatigue (RCF) damage was noted for the bainitic steel compared to head-hardened pearlitic steel. Kristen also stated that in the J6 bainitic low rail of the curve, cracks and shelling were almost completely absent, while for the pearlitic steel, widespread RCF damage, extensive cracks and shelling were observed. Although bainitic steels have shown superior performance, their application as premium rails has been hindered due to manufacturing and welding difficulties. Nevertheless, fundamental research into bainitic steels in comparison with premium

Keywords: bainitic steel, fracture toughness, fatigue, pearlitic steel.

This work was sponsored by the Federal Railroad Administration, Department of Transportation, under grant No. DTFR53-02-G-00021. The fracture toughness study was sponsored by the Y-12 security complex, through the PDRD program under subcontract No. 430003430.

pearlitic steels can elucidate the microstructural origin of mechanical properties, fracture toughness, and fatigue damage tolerance of these materials. This will lead to the development of rail steels with superior performance.

Pearlitic steels obtain their strength from fine grains of pearlite. However, there is a limit to the production of very fine grains in manufacturing and post-heat treatment processes. In contrast, bainitic steels derive their strength from ultra-fine structure with many dislocations that are harmless and confer high strength [Sawley 1997]. The microstructure of bainitic steel is a metastable aggregate of ferrite and cementite produced from the transformation of austenite at temperatures below the pearlite range and above the martensite starting temperature. Unlike the microstructure of pearlitic steel, the ferrite in bainitic steel has an acicular morphology and the carbides are discrete particles. The microstructure of bainitic steel is more complex than that of pearlitic steel and is largely dependent on the compositions and processing conditions. Bainite can be formed from austenite by isothermal transformation or by continuous cooling transformation (CCT). Usually, bainite in isothermally transformed steel is well characterized and distinguished as *upper bainite* and *lower bainite* depending on whether the carbides are distributed between individual ferrite regions or within them, respectively. The microstructure of upper bainite contains parallel lath-shape units of ferrite, which produce the so-called "feathery" appearance in optical microscopy and are formed at temperatures above 350° C. Lower bainite, on the other hand, has an acicular appearance similar to tempered martensite, and is often produced at temperatures below 350° C. These microstructural differences between upper and lower bainitic steel have led to differences in their mechanical properties. Usually, lower bainitic steel has higher strength and toughness than upper bainitic steel [Davis 1998].

A limited amount of research has so far been conducted on bainitic steels. Su and Clayton [1996] gave a review of experimental research on wheel-rail contact, pointing out that the study of bainitic rail steel remained a fertile area for research. They found that rolling contact fatigue cracks are associated with plastic deformation and embryo cracks even under dry running conditions. Jeong et al. [1998] have estimated rail wear limits based on rail strength investigations. Surface modification has been proposed to mitigate the wear and prevent the formation of surface cracks on the rails [Dimelfi et al. 1998; Yun et al. 1996]. Yokoyama et al. [2002] studied the effect of angle of attack ($1^\circ - 5^\circ$) on the RCF damage resistance of pearlitic and bainitic rail steels. They found that bainitic rail steel displayed better RCF damage resistance than pearlitic steel for all angles of attack tested. The RCF performance of low strength bainitic steel was higher than the head-hardened pearlitic rail steel. Very recently Li et al. [2006] studied the RCF of a medium carbon bainitic steel (0.43% carbon). Three stages of RCF short-crack kinetics were observed, similar to those for conventional long-crack fatigue. Vertical short cracks parallel to the axis of the roller were observed in the initial stage, followed by a stage of un-propagating behavior, which consumed a larger number of RCF cycles. In the third stage the vertical short cracks re-propagated with a high acceleration in the direction parallel to the contact surface. It was suggested that the number of RCF cycles at which the re-propagation of the vertical short cracks occur could be used as the crack initiation life of the RCF. At this point, typically, the RCF cracks are very small and the initiation life may not be a dominating factor and hence the crack growth life ought to be considered. Kang et al. [2006] studied the ratcheting behavior of the same bainitic steel. They found that the ratcheting strain strongly depends on the stress level. At a low stress level a constant ratcheting strain rate was reached. At higher stress

levels the evolution of ratcheting strain with the number of RCF cycles displayed three stages, in manner similar to those obtained for vertical short crack kinetics.

Orringer [1997; 1988] studied the fatigue crack propagation life of detail fracture in rails. More recently, Glowacki and Kuziak [1997] have investigated the effect of coupled thermal-mechanical processes on the evolution of microstructure in rails. Head hardening behavior and rolling contact fatigue have also been studied [Wong et al. 1996; Muster et al. 1996]. Fracture toughness and fatigue strength have been applied as criteria for characterization of the fatigue damage resistance of railway rails [Vitez 1997]. The limitations of fracture toughness and fatigue strength criteria are obvious due to the diversified composition of rails and the complicated live bending stress and shear stress, and residual stress conditions. Another factor that must be addressed is that data on rail flaw growth for lifetime estimates is insufficient, which makes it difficult to further understand the fatigue behavior and assess the fracture resistance of railway rail alloys under cyclic loading conditions. Thus, it is necessary to acquire more fatigue data, to study the related fracture and failure mechanism and to propose new criteria of damage tolerance for rail steel systems.

In the current study, the microstructure-properties relationships, plane strain fracture toughness, and fatigue crack growth of a J6 bainitic and a premium pearlitic rail steel are studied to gain fundamental understanding of the underlying mechanisms between these performance-related properties and the microstructure of the materials. ASTM standard E399A [ASTM 1983] is used to determine and compare the plane strain fracture toughness of the two materials. The fatigue crack growth behavior of the two steels generated by the current authors is correlated with plane strain fracture toughness data for the two materials.

2. Materials and experimental approach

Materials. The materials used in this study were a J6 bainitic rail steel and a premium pearlitic rail steel provided by the Transportation Technology Center, Inc., Pueblo, Colorado. Both rails were new and had not been placed in service. The premium pearlitic rail steel was manufactured by Rocky Mountain Steel Mills, Pueblo, Colorado in 1998. Although the exact composition of the rail used in the current investigation is not known, it is assumed to be within the composition range for pearlitic steel as controlled by the American Railway Engineering Manufacturing Association (AREMA). This range is presented in [AREMA 1997, Table 1]. No reported details on the manufacture of the J6 bainitic rail are available, but it is believed that no heat treatment was done. The composition of bainitic rail steel as determined by CMS Colorado Metallurgical Services (J. Kristan, private communication, 2003) is given in Table 1. According to Sawley and Kristan [2003], J6 bainitic steel has a carbide-free structure with lath ferrite and interlath austenite in the as-rolled condition.

Element	C	Mn	P	S	Si	Ni	Cr	Cu	Mo	V
Bainitic steel	0.23	1.93	0.012	0.008	1.96	0.14	1.84	0.13	0.43	0.007
Pearlitic steel	0.72~0.78	0.60~1.25	0.035	0.037	0.1~0.6	0.25	0.25~0.5		0.1	0.03~0.05

Table 1. Composition of the rail steels in percent by weight.

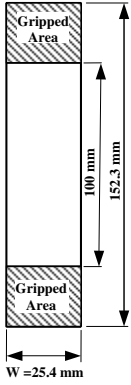
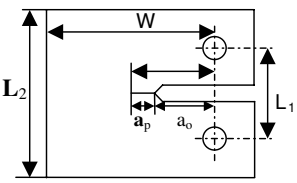
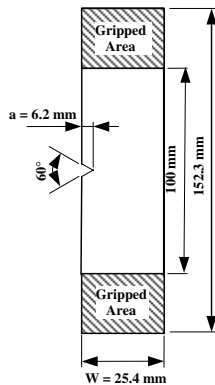
Mechanical Properties Rectangular	Fracture Toughness $\frac{1}{2}$ T compact tension	Fatigue Crack Growth Single edge notch
 <p>Thickness, $B = 2$ mm</p>	 <p> $W = 22.86$ mm $a_0 = 8.89$ mm $a_p = \text{pre-crack length}$ $L_2 = 27.43$ mm $L_1 = 13.97$ mm Pin diameter = 6.35 mm $B = 9.14$ mm </p>	 <p>$B = 2$ mm</p>

Figure 1. Specimen geometry.

Specimen geometry. All test specimens were cut from railheads along the direction of the rail using EDM (electric discharge machining). Samples were taken from the middle of the railheads in order to avoid top surface effects. This is especially important for the pearlitic railhead which has undergone head hardening by air quenching. The specimen geometries for each loading configuration are shown in Figure 1. The compact tension specimens were subjected to fatigue pre-cracking in order to introduce a sharp notch for the fracture toughness testing. An intended pre-crack length of about 2.5 mm was introduced into each specimen to have a target geometrical correction factor (a/W) of 0.5. Difficulties were encountered initially when attempting to pre-crack the bainitic samples and therefore they were stress relieved at 454° C for 1/2 hour prior to pre-cracking. This observation raises a question about the inherent residual stress in the bainitic rail steel. Further research on understanding the residual stress level in the bainitic rail steel is needed. All of the pearlitic steel samples pre-cracked in the normal fashion with relatively straight pre-cracks without additional treatment. For the purposes of calculation the actual crack length was measured from the fracture surface following the tests.

Experimental approach. For mechanical properties and fracture toughness studies, static tensile experiments were performed using an MTS 810 materials testing system equipped with a 100 kN load cell. The MTS is equipped with TestStar II software. Load was applied at a rate of 20 kN/min. The fracture toughness data were analyzed according to ASTM standard E399.

The fatigue tests were conducted at an ambient temperature of 25° C under load control conditions using a sinusoidal waveform and a frequency of 1 Hz. The maximum stress was 200 MPa, and the ratio of minimum stress to maximum stress was 0.1. The crack length at various intervals of number of cycles was recorded during the tests. A video camera with a zoom lens was used to view the crack tip region, measure the crack length and capture the damage associated with the crack growth. A total of three

samples were tested from each material, and data from each sample were used for the fatigue crack propagation analysis and the fatigue damage species examination.

The microstructures of the bainitic and the pearlitic rail steels were studied using an optical microscope. Various microstructural features of each rail steel were identified. The fracture surfaces for all specimens were examined using a Hitachi S-2150 Scanning Electron Microscope operated at acceleration voltage of 20 kV. Typical micrographs revealing the fracture surface morphology were taken using a PCI-Image Management System.

3. Results and discussion

Microstructural analysis. Figure 2 shows the optical microstructures of bainitic and pearlitic steels are shown in The bainitic microstructures (left) reveals a mixture of tempered martensite and ferrite associated with intralath carbides. The autotempered martensite is distinguished from the bainite by the precipitation of multiple, rather than single, cementite structures within each lath, very similar to those reported in [Bramfitt and Speer 1990]. Typical pearlitic microstructure with fine lamellar aggregate of very soft and ductile ferrite and very hard carbide cementite is shown in the right half of Figure 2. The lamellae are aligned in the same orientation in one grain. The properties of pearlitic steels are mainly determined by the spacing between the ferrite-cementite lamellae. The grains of bainitic steels are easy to see and the grain boundary is very thin. Optical measurements of the grain size of pearlitic and bainitic steels were taken using OLYMPUS GX51 Inverted System Metallurgical Microscope and software-PAX-IT5.2. Twenty grains were sampled to determine the average grain size. Three diagonal measurements were taken for each grain and an average grain size was obtained. A total average was obtained based on the twenty grains. The average grain size of bainitic steel is about $90\ \mu\text{m}$, while the average grain size of pearlitic steel is about $50\ \mu\text{m}$. The microstructure of bainite is more complex than that of pearlite because of the wide range of cooling rates.

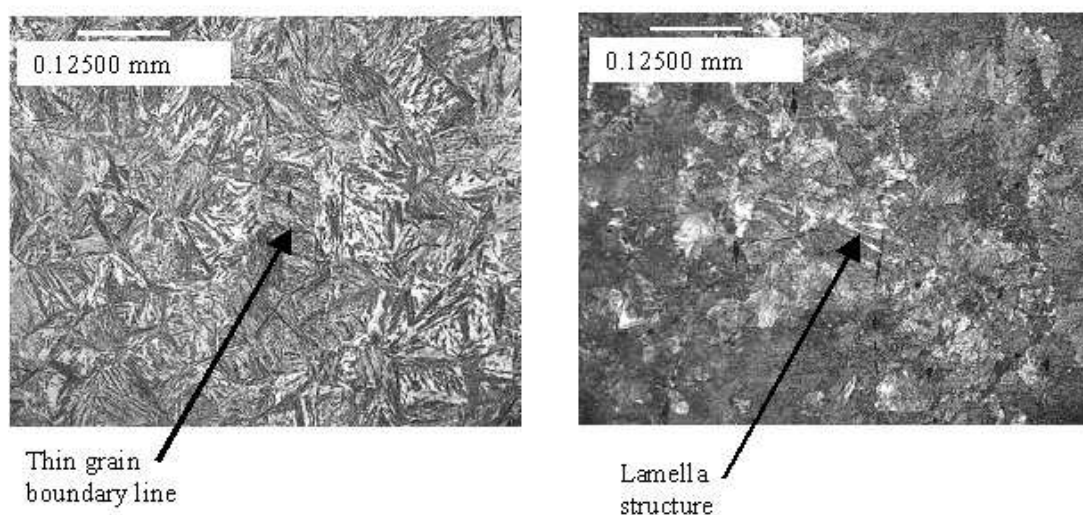


Figure 2. Optical microstructures of rail steels: (left) bainitic, (right) pearlitic.

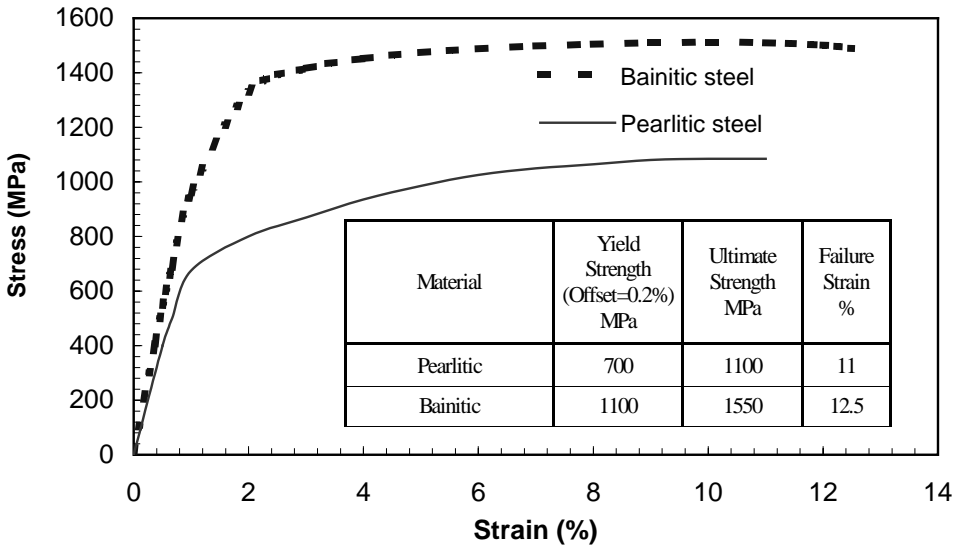


Figure 3. Stress-strain relationships of pearlitic and bainitic rail steels.

Stress-strain relationships. The stress-strain relationships of bainitic and pearlitic rail steels based on unnotched specimens are shown in Figure 3. It can be seen that the ultimate strength, yield strength and strain to failure of bainitic steel are higher than that of pearlitic steel. The stress is calculated based on the original cross-sectional area before testing. A summary of these mechanical properties for J6 bainitic rail steel and a premium pearlitic rail steel are also given in Figure 3. There is an increase of about 36% in the ultimate strength, 77% in the yield strength and 15% in the strain to failure from the pearlitic to the bainitic rail steel. The higher strength of the J6 bainitic steel can be related to the distribution of carbide particles. Strength increases with increasing number of carbide particles per unit area in the plane of the section. By decreasing the bainite transformation temperature, the carbides will be dispersed, the size of carbide particles will be smaller, and the number of carbide particles in the plane of section will be large. Thus, the strength will increase greatly.

Fracture toughness evaluation. The general expression of the plane strain fracture toughness for a compact tension specimen used to compare the two rail steels is

$$K_1 = \frac{P}{B\sqrt{W}} f\left(\frac{a}{W}\right), \tag{1}$$

where P is the load, B is the thickness, W is the distance from the center of the loading holes to the edge of the specimen, a is the total crack length (initial plus pre-crack), and $f(a/W)$ is a geometrical correction factor. The geometrical correction factor, (a/W) , in Equation (1) can be expressed as a function as follows [Srawley 1976; Newman 1974]:

$$f\left(\frac{a}{W}\right) = \frac{\left(2 + \frac{a}{W}\right) \left[0.886 + 4.64\left(\frac{a}{W}\right) - 13.32\left(\frac{a}{W}\right)^2 + 14.72\left(\frac{a}{W}\right)^3 - 5.6\left(\frac{a}{W}\right)^4\right]}{\left(1 - \frac{a}{W}\right)^{3/2}}$$

The bainitic steel demonstrated elastic behavior and cleavage fracture. Therefore ASTM Standard E399 was used for the analysis. The data for all three samples tested along with their calculated values of K_{Ic} based on Equation (1) are presented in Table 2. To validate the calculated value of K as a true K_{Ic} fracture toughness, the following conditions must be met:

$$a \text{ and } B \geq 2.5(Kq/\sigma_y)^2, \quad P_{\max}/P_q < 1.1. \tag{2}$$

For the bainitic steel, the value of $2.5(Kq/\sigma_y)^2 = 2.5(52/1100)^2 * 1000 = 2.24$ mm. This value is less than B , which is 9.14 mm, and less than a which is about 12 mm. Therefore, the first condition in Equation (2) is met. In addition P_{\max} equals P_q , thus also meeting the second condition. Therefore these fracture tests for the bainitic steel yield a valid value of K_{Ic} according to ASTM E399. The average value of K_{Ic} for the bainitic steel was found to be 52 MPa \sqrt{m} .

The pearlitic steel also demonstrated elastic behavior and cleavage fracture. Similarly ASTM Standard E399 was used for the analysis of the plane strain fracture toughness, K_{Ic} . The data for all three premium pearlitic steels samples tested along with their calculated values of K_{Ic} based on Equation (1) are also presented in Table 2. For the pearlitic steel we have $2.5(Kq/\sigma_y)^2 = 2.5(41/700)^2 * 1000 = 8.6$ mm. This value is less than B , which is 9.14 mm and less than a , which is about 12 mm; this meets the first condition in Equation (2). In addition P_{\max} equals P_q , so the second condition is met. Therefore these fracture tests for the pearlitic steel yield a valid value of K_{Ic} according to ASTM E399. The average value of K_{Ic} was found to be 41 MPa \sqrt{m} for the premium pearlitic steel.

Based on the plane strain fracture toughness analysis using compact tension specimens the fracture toughness of the bainitic steel was found to be about 27% higher than that of the premium pearlitic steel.

Sample	W (mm)	a_o (mm)	a_p (mm)	a (mm)	(a/W)	$f(a/W)$	P_m (kN)	P_q (kN)	B (mm)	Kq (MPa \sqrt{m})	K_{Ic} (MPa \sqrt{m})
Bainitic Rail Steel											
#1	22.4	8.89	3.0	11.89	.531	10.66	6.6	6.6	9.14	51.43	51.43
#2	22.4	8.89	3.5	12.39	.553	11.48	6.3	6.3	9.14	52.87	52.87
#3	22.6	8.89	3.4	12.29	.544	11.13	6.4	6.4	9.14	51.44	51.44
											(average) 52
Pearlitic Rail Steel											
#1	22.4	8.89	3.2	12.09	.540	10.98	5.7	5.7	9.14	45.75	45.75
#2	22.3	8.89	3.3	12.19	.547	11.25	4.7	4.7	9.14	38.74	38.74
#3	22.4	8.89	3.7	12.19	.562	11.85	4.3	4.3	9.14	37.25	37.25
											(average) 41

Table 2. Compact tension specimen geometry and test results for bainitic and pearlitic steels. Notation: W is the distance from the center of the loading holes to the edge of the specimen, a_o the initial machined notch length, a_p the fatigue pre-crack, a the total crack length, P_m the maximum load, P_q the load at which K_q is calculated, B the thickness, K_q the stress intensity factor calculated from Equation (1), and K_{Ic} the mode I fracture toughness.

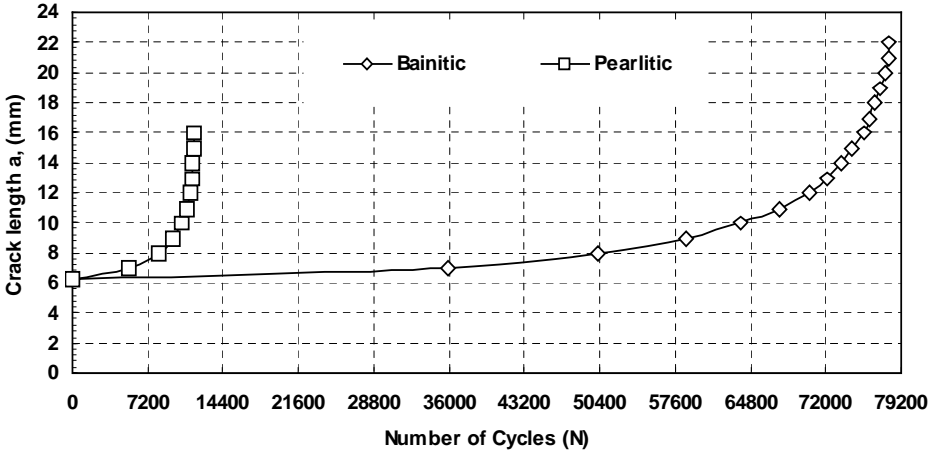


Figure 4. Fatigue crack length, a , versus the number of cycles, N .

Fatigue crack growth analysis. Figure 4 shows the average crack length a versus the number of cycles N , for both bainitic and pearlitic rail steel. We see that the total fatigue lifetime of bainitic steel is much higher than that of pearlitic steel. This is based on the average of three macroscopically identical specimens from each material. The total average fatigue lifetime for the bainitic and pearlitic steel samples is about 78000 and 11000 cycles, respectively. We also see that both initiation lifetime and propagation lifetime for the bainitic steel is higher than that for the pearlitic. The slopes of the curves in Figure 4 are taken as the average crack speed at each crack length.

The potential energy P , was calculated from the hysteresis loops recorded at intervals of number of cycles. It is the area above the unloading curve at each crack length. On this basis, the relationship

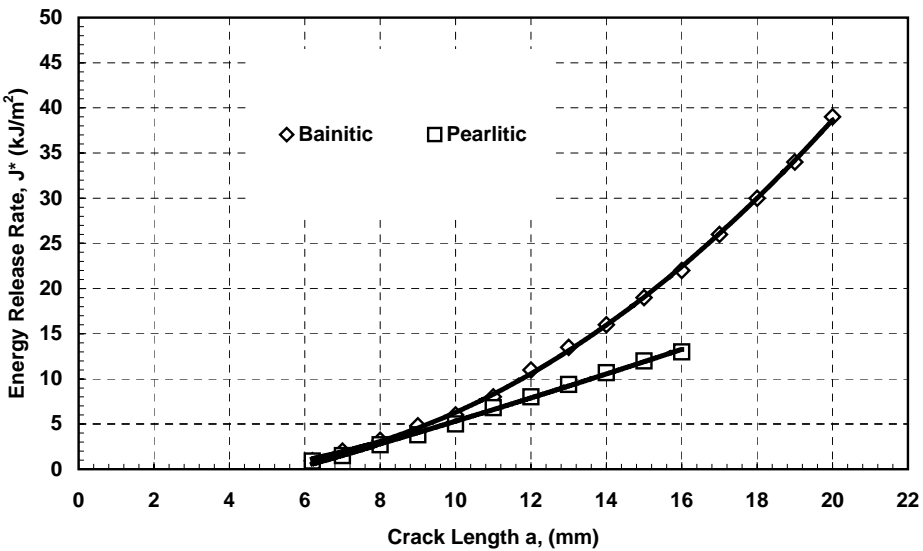


Figure 5. Energy release rate, J^* , versus the fatigue crack length, a .

between the potential energy and the fatigue crack length a , was established. The energy release rate J^* from the potential energy curve is based on

$$J^* = \frac{1}{B} \frac{\partial P}{\partial a},$$

where P is the potential energy, a is the crack length and B is the specimen thickness. Figure 5 illustrates the average energy release rate, J^* , as a function of the crack length a , for the bainitic and pearlitic rail steels. The value of J^* increases with the increase of the crack length a . The critical value of J^* for the bainitic steel is about 40 kJ/m², while that for the pearlitic steel is about 13 kJ/m². This is the point where the onset of rapid crack growth is observed. The ratio between the critical crack length and specimen width ($\frac{a_c}{W}$) is higher for bainitic steel than that for pearlitic steel. The values of the ratio a_c/W are 0.8 and 0.63 for bainitic and pearlitic steels respectively.

The crack speed versus the energy release rate J^* for both bainitic and pearlitic rail steel are shown in Figure 6. The crack deceleration in the case of the bainitic steel started after a value of J^* of about 10 kJ/m². This is indicative of material damage ahead of the crack tip. It can also be seen from the figure that the first stage, or initiation stage, of fatigue crack propagation (FCP) kinetics is well developed in the bainitic steel, while that for the pearlitic is less pronounced. Under the same J^* , the crack growth rate of pearlitic steel is higher than that of bainitic steel, which means that bainitic rail steel has higher resistance to FCP.

Fracture surface morphology examination was performed on typical fatigue-failed specimens of each material to identify the fatigue damage species. Micrographs (1000X) taken from the stable crack propagation region, ahead of the notch tip, are shown in Figure 7 for the bainitic and pearlitic rail steels respectively. Ductile tearing, and extensive ridge formation are associated with the bainitic steel (left); pulled-up pearlite lamella, microcracks and micro-void coalescence can be found in the pearlitic steel

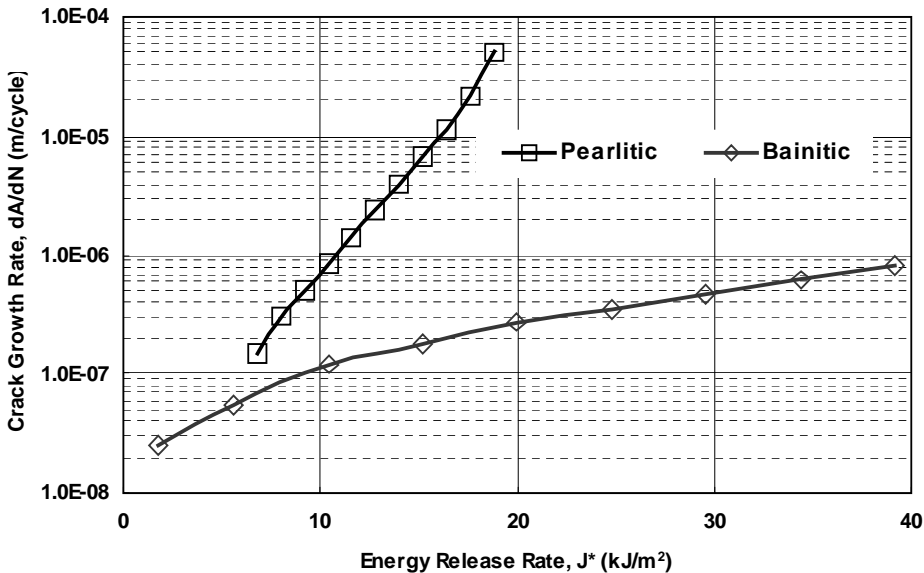


Figure 6. Crack growth rate, da/dN , versus energy release rate J^* .

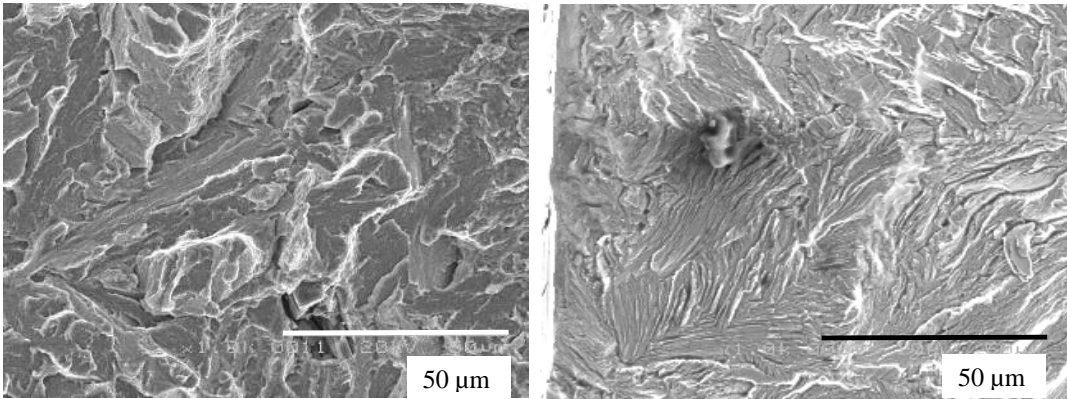


Figure 7. SEM micrographs at 1000X taken from the beginning of the stable crack propagation region: (left) bainitic and (right) pearlitic steels.

(right). In general, these features reflect the crack deceleration and indicate a considerably high energy consuming process associated with the crack propagation. It appears to be the case that the bainitic rail steel displays more ductile fracture features in the stable region than the pearlitic steel.

To identify the microstructural origin of higher fracture toughness and fatigue damage tolerance of the bainitic rail steel as compared to pearlitic steel, we examine the optical micrograph of the pearlitic rail steel in Figure 8, which displays pearlitic colonies. The lamella structure is clearly visible. The properties of pearlitic steel are mainly determined by the spacing between the ferrite-cementite lamella shown in this grain [Aglan et al. 2004]. It has been stated [Yokoyama et al. 2002] that the lamella structure causes anisotropy in the physical and mechanical properties of the pearlitic steel, depending on lamella orientation. Under plastic deformation, high stress concentration can occur at the colony boundaries and cause cracking along these boundaries. The bainitic microstructure as seen in Figure 2 (left) does not

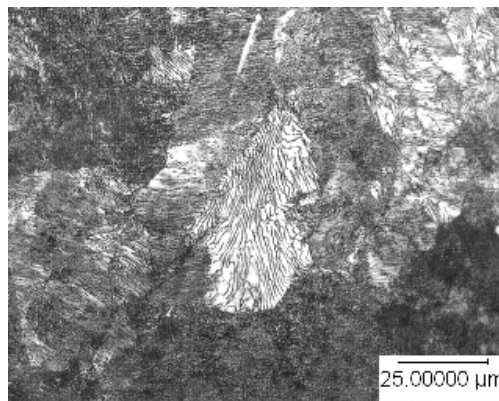


Figure 8. Optical micrograph of pearlitic railsteel showing the lamella structure in a pearlitic colony.

show strong microstructural anisotropy, reducing the crack initiation and growth sites. It is believed that this behavior is responsible for the higher fracture toughness and fatigue damage tolerance of the bainitic steel in comparison with pearlitic steels. This can also explain the better RCF damage resistance of the bainitic steel in comparison with pearlitic steel.

4. Conclusions

Based on the testing of the rail steels and the related data analyses, the following conclusions are drawn:

1. The microstructure of J6 bainitic rail steel is more complex than that of pearlitic steel. The average grain size of bainitic rail steel is about $90\ \mu\text{m}$ while that for pearlitic rail steel is about $50\ \mu\text{m}$. The J6 bainitic steel has ultimate strength, yield strength and elongation to failure of about 1500 MPa, 1100 MPa and 13% respectively. These values are higher than those for pearlitic steel.
2. Fracture toughness evaluation was conducted using $(1/2T)$ compact tension specimens according to ASTM standard E399. It was found that the average K_{Ic} for the bainitic rail steel is $52\ \text{MPa}\sqrt{m}$, while that of the premium pearlitic steel is $41\ \text{MPa}\sqrt{m}$.
3. Crack speed for the bainitic steel is lower than that for the pearlitic steel over the entire range of the energy release rate. The bainitic steel exhibits a higher rate of crack deceleration in the second stage, as indicated by the lower slope of the FCP curve in comparison with pearlitic steel. This indicates the superior resistance of bainitic rail steel to FCP, that is, higher fatigue damage tolerance. This is in agreement with the plane strain fracture toughness data for the two materials.
4. Ductile tearing and extensive ridge formation are associated with the stable crack propagation region of the bainitic steel. Pulled-up pearlitic lamella, limited microcracks and micro-void coalescence can be found in the pearlitic steel. The more ductile features of the bainitic steel reflect the crack deceleration and indicate a considerably higher energy-consuming process giving it its superior fracture and fatigue crack propagation resistance.

References

- [Aglan et al. 2004] H. A. Aglan, Z. Y. Liu, H. M. F., and M. Fateh, "Mechanical and fracture behavior of bainitic rail steel", *J. Mater. Process. Technol.* **151**:1–3 (2004), 268–274.
- [AREMA 1997] *AREMA manual for railway engineering*, 4, American Railway Engineering Manufacturing Association, 1997.
- [ASTM 1983] ASTM, "Standard test method for fracture toughness of metallic materials", Technical Report E 399-90, American Society for Testing and Materials, Philadelphia, 1983.
- [Bramfitt and Speer 1990] B. L. Bramfitt and J. G. Speer, "Perspective on the morphology of bainite", *Metall. Trans. A* **21** (1990), 817–829.
- [Davis 1998] J. R. Davis (editor), *Metals handbook, desk edition*, 2nd ed., ASM International, Materials Park, OH, 1998.
- [Davis et al. 2002] D. Davis, C. Sasaoka, S. Singh, and D. Guillen, "Advanced design of bainitic steel rail crossing diamond under HAL service", Technical Report TD-02-024, Transportation Technology Center, Pueblo, CO, 2002.
- [Dimelfi et al. 1998] R. J. Dimelfi, P. G. Sanders, B. Hunter, J. A. Eastman, K. J. Sawley, K. Leong, and K. J., "Mitigation of subsurface crack propagation in railroad rails by laser surface modification", *Surf. Coat. Technol.* **106**:1 (1998), 30–43.
- [Glowacki and Kuziak 1997] M. Glowacki and R. Kuziak, "Application of coupled thermal-mechanical model to the numerical analysis of the microstructure development during rolling and air-cooling of rails", pp. 1313–1316 in *Fifth International Conference on Computational Plasticity* (Barcelona, 1997), edited by D. R. J. Owen et al., Pineridge, Swansea, 1997.

- [Jeong et al. 1998] D. Jeong, Y. Tang, and O. Orringer, "Estimation of rail wear limits based on rail strength investigations", Technical Report DOT/FRA/ORD-98/07, Federal Railroad Administration, Office of Research and Development, Washington, DC, 1998.
- [Kang et al. 2006] G. Z. Kang, Y. Li, Y. Gao, Q. Kan, and J. Zhang, "Uniaxial ratcheting in steels with different cyclic softening/hardening behaviours", *Fatigue Fract. Eng. Mater. Struct.* **29**:2 (2006), 93–103.
- [Kristan 2005] J. Kristan, "R&T results of AAR developed J6 bainitic type rail steel", TTCI Technology Digest TD-05-014, Transportation Technology Center, Pueblo, CO, 2005.
- [Li et al. 2006] Y. Li, G. Kang, C. Wang, P. Dou, and J. Wang, "Vertical short-crack behavior and its application in rolling contact fatigue", *Int. J. Fatigue* **28**:7 (2006), 804–811.
- [Muster et al. 1996] H. Muster, H. Schmedders, K. Wick, and H. Pradier, "Rail rolling contact fatigue: the performance of naturally hard and head-hardened rails in track", *Wear* **191**:1–2 (1996), 54–64.
- [Newman 1974] J. E. Newman, "Stress analysis of compact specimens including the effects of pin loading", pp. 105–121 in *Fracture analysis: proceedings of the 1973 National Symposium on Fracture Mechanics, II* (College Park, MD, 1973), edited by G. R. Irwin, ASTM Special Technical Publication **560**, ASTM, Philadelphia, 1974. Paper ID STP33136S.
- [Orringer 1988] O. Orringer, "Crack propagation life of detail crack fractures in rails", Technical report, Volpe Transportation Systems Center Report, 1988.
- [Orringer et al. 1997] O. Orringer et al., "Risk/benefit assessment of delayed action concept for rail inspection", Technical Report DOT/FRA/ORD-99/03 DOT-VNTSC-FRA-99-7, Federal Railroad Administration, Office of Research and Development, Washington, DC, 1997.
- [Sawley 1997] K. J. Sawley, "Bainitic steels for rails", Technical Digest TD97-001, Transportation Technology Center, Pueblo, CO, 1997.
- [Sawley and Kristan 2003] K. Sawley and J. Kristan, "Development of bainitic rail steels with potential resistance to rolling contact fatigue", *Fatigue Fract. Eng. Mater. Struct.* **26**:10 (2003), 1019–1029.
- [Smith 2004] W. F. Smith, *Foundations of materials science and engineering*, 3rd ed., McGraw-Hill, New York, 2004.
- [Srawley 1976] J. E. Srawley, "Wide range stress intensity factor expressions for ASTM E399 standard fracture toughness specimens", *Int. J. Fract. Mech.* **12**:3 (1976), 475–476.
- [Su and Clayton 1996] X. Su and P. Clayton, "Surface-initiated rolling contact fatigue of pearlitic and low carbon bainitic steels", *Wear* **197**:1–2 (1996), 137–144.
- [Vitez 1997] I. Vitez, "The fracture toughness and the fatigue strength of railway rails", *Int. J. Fatigue* **19**:10 (1997), 734–734.
- [Wong et al. 1996] S. L. Wong, P. E. Bold, M. W. Brown, and R. J. Allen, "A branch criterion for shallow angled rolling contact fatigue cracks in rails", *Wear* **191**:1–2 (1996), 45–53.
- [Yokoyama et al. 2002] H. Yokoyama, S. Mitao, S. Yamamoto, and M. Fujikake, "Effect of the angle of attack on flaking behavior in pearlitic and bainitic steel rails", *Wear* **253**:1–2 (2002), 60–66.
- [Yun et al. 1996] X. Yun, D. B. Bogy, and C. S. Bhatia, "Wear of hydrogenated carbon coated disks by carbon coated and uncoated Al₂O₃/TiC sliders in ultra high vacuum", *IEEE Trans. Magn.* **32**:5 (1996), 3669–3671.

Received 18 Jun 2006. Accepted 15 Sep 2006.

HESHMAT A. AGLAN: aglanh@tuskegee.edu

College of Engineering, Architecture, and Physical Sciences, 218 Foster Hall, Tuskegee University, Tuskegee, AL 36088, United States

MAHMOOD FATEH: mahmood.fateh@dot.gov

Federal Railroad Administration, 1120 Vermont Ave., Washington, DC 20590, United States